electronics

MDPI

Article

An Enhanced Multiscale Retinex, Oriented FAST and Rotated BRIEF (ORB), and Scale-Invariant Feature Transform (SIFT) Pipeline for Robust Key Point Matching in 3D Monitoring of Power Transmission Line Icing with Binocular Vision

Nalini Rizkyta Nusantika, Jin Xiao * and Xiaoguang Hu

State Key Laboratory of Virtual Reality Technology and Systems, School of Automation Science and Electrical Engineering, Beihang University, Beijing 100191, China; nusantikanalini@buaa.edu.cn (N.R.N.); xiaoguang@buaa.edu.cn (X.H.)

* Correspondence: xiaojin@buaa.edu.cn; Tel.: +86-10-82339780

Abstract: Power transmission line icing (PTLI) poses significant threats to the reliability and safety of electrical power systems, particularly in cold regions. Accumulation of ice on power lines can lead to severe consequences, such as line breaks, tower collapses, and widespread power outages, resulting in economic losses and infrastructure damage. This study proposes an enhanced image processing pipeline to accurately detect and match key points in PTLI images for 3D monitoring of ice thickness using binocular vision. The pipeline integrates established techniques such as multiscale retinex (MSR), oriented FAST and rotated BRIEF (ORB) and scale-invariant feature transform (SIFT) algorithms, further refined with m-estimator sample consensus (MAGSAC)-based random sampling consensus (RANSAC) optimization. The image processing steps include automatic cropping, image enhancement, feature detection, and robust key point matching, all designed to operate in challenging environments with poor lighting and noise. Experiments demonstrate that the proposed method significantly improves key point matching accuracy and computational efficiency, reducing processing time to make it suitable for real-time applications. The effectiveness of the pipeline is validated through 3D ice thickness measurements, with results showing high precision and low error rates, making it a valuable tool for monitoring power transmission lines in harsh conditions.

Keywords: power transmission line icing (PTLI); 3D monitoring; key point matching; binocular vision; multiscale retinex (MSR); ORB-SIFT; MAGSAC; RANSAC optimization; ice thickness estimation

check for updates

Citation: Nusantika, N.R.; Xiao, J.; Hu, X. An Enhanced Multiscale Retinex, Oriented FAST and Rotated BRIEF (ORB), and Scale-Invariant Feature Transform (SIFT) Pipeline for Robust Key Point Matching in 3D Monitoring of Power Transmission Line Icing with Binocular Vision. *Electronics* **2024**, *13*, 4252. https://doi.org/10.3390/electronics13214252

Academic Editor: Jenhui Chen

Received: 16 September 2024
Revised: 19 October 2024
Accepted: 28 October 2024
Published: 30 October 2024

Copyright: © 2024 by the authors. Licensee MDPI, Basel, Switzerland. This article is an open access article distributed under the terms and conditions of the Creative Commons Attribution (CC BY) license (https://creativecommons.org/licenses/by/4.0/).

1. Introduction

Power transmission line icing (PTLI) is an important issue that affects the reliability and safety of power grid systems, especially in cold regions. PTLI occurs through the ice phenomenon, in which cold water droplets increase on the transmission line and then gradually freeze to become a layer of ice on top of the line cables, conductors, insulators, and supporting structures. The formation of this ice sheet can result in a series of significant problems, such as line breaks, tower collapses and other power transmission damage, which is a very dangerous threat to the safety of electric power operating systems. Worse, seriously threatening reliability, PTLI also brings great economic losses to the company and security risks to the country and society. In addition to the technical problems it causes, the impact of the ice sheet on transmission lines is very wide. Ice loads on various components of the power transmission system cause high losses for utility companies, and repairing damaged systems is also very expensive. In addition, PTLI disasters have an impact on the instability of the power supply system, which often leads to regional power outages and, thus, affects human activities and poses a significant risk to infrastructure [1–3]. Between 1980 and 2000, major snowstorms caused damage to transmission lines in several cities

in the United States, the United Kingdom, Canada, Russia, and Norway, creating global problems. In China, large-scale power outages occurred in 2005 and 2008 due to PTLI disasters that caused a major impact on the power grid and beneficiaries suffered huge economic losses [1].

Similarly, an ice storm hit the eastern province of Canada in 2013, damaging $200 million worth of property. The PTLI disaster left more than a million of its consumers in the dark for several days. For example, three 500 kV transmission lines covering the 500 kV Guanli line, the 500 kV Dushan line, and the 500 kV Guanqiao line were tripped and disconnected in January 2018 due to melting ice and tremors in the Anhui province, which posed a severe danger to the safe operation of the power grid [4–6]. The PTLI disaster also occurred in February 2021 and affected the power grid system in Texas, U.S., leaving millions of people without electricity during winter. Since February 2024, the city of Wuhan in Hubei province has been hit by a low-temperature freezing rain disaster, which refers to freezing rain that causes difficulties in transportation and electricity in the region. Based on the problems mentioned above, it is necessary to monitor the level of ice accumulation in power transmission lines to prevent damage to infrastructure and also provide support for a consistent and stable power supply in areas experiencing extreme and bad weather conditions [7].

Processing data from PTLI images is not easy; PTLI environments usually show climate change and irregular light conditions, leading to noise and artifacts in the images taken [8,9]. In the context of improving the accuracy of 3D measurements and monitoring of power transmission lines for ice thickness, such conditions can lead to poor image quality, which makes it difficult to identify and analyze some image features, such as low contrast as a result of inadequate lighting or visibility barriers as exemplified by snow or ice sheets, which can make it difficult to use signal processing approaches for image enhancement. The difficulties mentioned above can be critical in applications where accuracy is most important, for example, in 3D measurements, so it can lead to incorrect judgment and inaccurate image processing. According to the above description, one of them is to create an effective and powerful image processing algorithm to support a significant range of monitoring and measurement work under suboptimal environments [10,11].

Generally, 3D measurements on PTLI consist of several key stages [2,12]. The first stage is PTLI identification, where edge detection and line detection are performed to identify the contours and main geometric structures of objects in 3D space. Once the ice is identified, the next stage is key point matching, in which key point matching matches unique points, such as angles or texture features, which can be recognized on two images from different angles of view (left and right). The matching points on both images are used to calculate depth or 3D information through triangulation. With key point matching, the system can determine the 3D coordinates of each of those unique points in 3D space, which is essential for reconstruction accuracy. Once the 3D model is formed, ice thickness measurements can be made based on the results of the 3D reconstruction. However, this paper only focuses on the improvement of the key point-matching stage. Key point matching is an important stage in 3D reconstruction, as accuracy depends on the success of key point detection and key point matching. In some cases, this key point matching process has environmental disturbances that cause image degradation, such as noise, background, and low lighting problems. It is generally noted that failed key point matching methods in PTLI images resulted in the desired decrease in accuracy and durability. The above limitations are the reason why better methods are needed to find and match important points in difficult environmental conditions. Improving the accuracy and reliability of key point matching is important to improve the effectiveness of image processing in the application of ice thickness and the effectiveness of the methods used in the monitoring process. In this study, key point matching is used in PTLI monitoring applications where information is considered based on ice thickness measurements, so an accurate key point matching method is needed.

The primary objective of this research is to develop a robust image processing pipeline capable of accurately detecting and matching key points between images in challenging environments. The pipeline is designed for PTLI 3D monitoring based on binocular vision. The contributions of the research are as follows:

- The new integration for 3D measurement: the research combines established techniques like multiscale retinex (MSR) and contrast limited adaptive histogram equalization (CLAHE); oriented FAST and rotated BRIEF (ORB); and scale-invariant feature transform (SIFT) in a new method. This integration into a cohesive pipeline specifically targets robust key point matching. The application of these new methods to the PTLI image allow for 3D measurements for ice thickness estimation;
- Advanced random sample consensus (RANSAC)-based refinement with m-estimator sample consensus (MAGSAC) Integration: MAGSAC-driven RANSAC optimization with iterative parameter tuning and least median of squares (LMEDS) integration for superior outlier exclusion and transformation accuracy;
- Automatic cropping and practical application: The automatic cropping mechanism is based on the improvement of a connected component analysis, coupled with practical application and validation in PTLI images.

2. Literature Review

2.1. Existing Key Point Detection and Matching Techniques

Image feature matching is one of the fundamental operations in image processing, used in a variety of vision and robotics applications such as stereo matching, image mosaic, specific object recognition, feature-based robot localization, and simultaneous localization and mapping, among others. ORB (oriented FAST and rotated BRIEF) and SIFT (scale-invariant feature transform) stand out for their distinctive strength and wide adoption. Rublee et al. proposed the oriented FAST and rotated BRIEF algorithm, which combines the FAST and BRIEF algorithms, making it a feature detector and a feature descriptor [13,14]. The length of an ORB feature descriptor is generally a binary string of 128, 256, or 512. ORB's contribution is to add a fast and accurate directional component to the FAST and efficient calculation for the BRIEF feature so that it can realize real-time calculations. However, it is not scale invariant and is sensitive to brightness. Lowe et al. proposed the well-known scale-invariant feature transformation (SIFT) algorithm. SIFT is a feature detector and a feature descriptor. The algorithm is theoretically not variable in scale and has good anti-interference to illumination, rotation, scaling, noise, and occlusion properties. The SIFT feature descriptor is a 128-dimensional vector. However, the calculation process of this algorithm is complicated, and the speed is slow [15,16].

Bay et al. proposed speeded-up robust features (SURF) [17,18]. SURF is a fast, high-performance, invariant scale and rotation invariant feature detector and descriptor that combines the Hessian matrix and the Haar wavelet. The SURF descriptor uses only 64-dimensional vectors, which reduces the time required for feature calculation and matching. Leutenegger et al. proposed a binary robust invariant scalable key points (BRISK) algorithm [19,20]. The BRISK algorithm typically uses the FAST algorithm to quickly detect the feature points of an image, then individually takes a grayscale sample of each key point environment and derives a 512-bit binary code by comparing the grayscale taken sample. BRISK has low computational complexity, good real-time performance, scale invariance, rotation invariance, and anti-noise ability, but it has poor matching accuracy. However, if some of the above methods are applied to PTLI images, problems remain, such as high noise levels, low lighting, and weather conditions. These can be problematic in detecting and matching key points, which is especially important in object recognition and 3D reconstruction. Therefore, a combined arrangement of the detector point method is necessary because the individual detectors may not be as effective in PTLI images due to the variation of the key points in different images.

2.2. Image Enhancement Techniques in Computer Vision

Image enhancement techniques are an important part of the success of image processing methods, especially in images where image quality is compromised by poor conditions such as poor lighting and high noise levels. Image enhancement aims to improve the visibility and detection of important image features to produce more accurate point detection and key point matching. One of the most effective methods of image enhancement is multiscale retinex (MSR), which is designed to mimic the ability of human visual systems to understand the details of objects in images with a wide dynamic range. The multiscale retinex (MSR) method combines single-scale retinex (SSR) with several scales. The MSR method improves noise reduction and improves detail. However, it has limitations regarding noise cancellation and can induce halo effects and distort colors along the boundaries of objects or high-contrast images [21–24].

The histogram equalization (HE) method is one of the oldest methods for enhancing an image contrast in general. This one normalizes the grayscale histogram to ensure that the result of the image processing will have a range of the possible intensity of shade of gray. However, the following are the disadvantages of this method. They do not take into consideration the local variations. In doing this, the adaptive histogram equalization (AHE) eliminates the problem by computing the individual HE transfer function for each pixel by looking at the gray values in the rectangular filter window around each pixel. Due to these issues, AHE might have the problem of amplifying noise, so, Pizer et al. introduced contrast-limited adaptive histogram equalization (CLAHE) [25,26]. Similar to the previous technique, CLAHE is also used to enhance local contrast in an image, and hence, it minimizes the problem of noise amplification [27]. CLAHE works by partitioning the image into various small segments, which are then given an equal distribution of intensity histogram. However, a limiting factor to the contrast enhancement is employed. This method is most suitable in the image, which needs enhancement in the fine detail as a parameter.

Other image enhancement techniques are unsharp masking, which enhances the image by increasing high-frequency images, and denoise wavelet, which reduces the noise content by converting the image into wavelet domain and then mining the wavelet coefficient. Bilateral filtering also has to be added as it is specifically good at blurring the images but preserving their edges, which can be useful for scenarios where the target imagery needs to be denoised while the edges are retained. The integration of this image enhancement method is crucial in creating a robust image processing method that can operate effectively in degraded conditions. Improved input image quality enables more accurate and reliable key point detection and key point matching, which is critical for applications such as 3D reconstruction of challenging PTLI images.

2.3. Applications in 3D Measurement of Ice Thickness

The 3D reconstruction application for PTLI monitoring on power transmission lines is important, where accurate monitoring is crucial to maintain system safety and efficiency. Current 3D reconstruction methods often rely on techniques such as stereo vision, structured light, or time-of-flight sensors, which use the principle of triangulation to reconstruct the 3D geometry of an object. For example, a stereo vision system uses two cameras to capture images from different angles. Then, point detection and key point matching from the images are carried out to estimate the depth and reconstruct the object in 3D. However, the accuracy of the stereo system is highly dependent on the proper key point matching. The challenges in the key point matching process are low lighting conditions, reflective surfaces, or repetitive textures. The goal of 3D reconstruction is to build accurate image mapping from different perspectives, which requires identifying and matching relevant key points in the image. Mismatches of key points in the homography will cause deviations in the 3D position [2,12,28].

Similarly, ice thickness calculations on power transmission lines also depend on accurate detection and measurement of ice accumulation from the PTLI images. Critical points

are detected and matched to align images taken at the same time and from different angles, making it possible to take measurements of ice thickness [29,30]. However, 3D reconstruction often faces difficulties, such as low illumination, the color of ice accumulation on the transmission line being the same as the background, and the complex background. These problems can affect the detection and matching of key points, which will directly affect the accuracy of the ice thickness measurement. For example, low illumination can result in the number of key points not being detected, which is insufficient for 3D reconstruction and causes the 3D model to be inaccurate. Noise or occlusion can further interfere with key point matching, which compromises the results of ice thickness measurements. A robust image processing scheme that can function effectively even in challenging environments for key point matching is proposed in this study. Improvement of the image processing method and combination of multiple key point matching algorithms aim to significantly improve the accuracy of 3D reconstruction and ice thickness estimation.

3. Methodology

3.1. Pipeline Overview

This research proposes to build an effective image processing system that would help identify the correspondence between images and their key points within PTLI images. The image processing pipeline comprises several steps, and each step is designed to solve particular problems that are usually encountered in image processing. The process starts with the image being loaded and preprocessed. At this stage, the image is read and set for analysis to change the format to standard and initial scaling. The following step is an image enhancement, which is useful for improving image resolution and erasing out noise, so that features can be easily detected. At this stage, methods for enhancing the visibility and contrast of the image are incorporated.

Subsequently, there will be an automatic cropping of the imagery stage that will focus on important parts of the images while eliminating unnecessary areas. The feature point detection is carried out after the image cropping; in this process, significant points called feature points and crucial descriptors for robust image matching are obtained. For feature detection, the ORB and SIFT algorithms detect the key points, after which feature matching matches the corresponding images. The next step is feature matching, with the intention of identifying the corresponding point between two images based on the key points. Following this stage, the RANSAC-based refinement is performed to select key point matching, eliminate outliers, and determine robust transformations between images. Finally, the points of interest are presented to assess the pipeline implementation and the correctness of the outputs. Figure 1 shows the block diagram of the proposed image processing pipeline.

3.2. Image Loading and Preprocessing

At this stage, efficient image acquisition and preprocessing are presented, consisting of several stages: color space standardization and computationally optimized rescaling. The loading and preprocessing stages of the image are very important so that the image is in a very good condition for processing. The loading step is to choose the file format, which is important because it affects the quality and ease of manipulating the image. Preprocessing also involves operations such as converting the images from BGR format to RGB format since they are compatible with most libraries and image processing procedures that involve matrices, and simpler analysis involves the transformation of the images from RGB into matrices of lower dimensions. The second one is a resizing process, and the image is resampled on the predefined scale factor, so it is not very computationally intensive. This step is beneficial to handle large datasets or real-time systems where concern for speed matters most. This step ensures that the necessary qualities of the image, such as the resolution and format of the image, are similar to the other images in the set of data collection as a solid basis for the next task in processing the image.

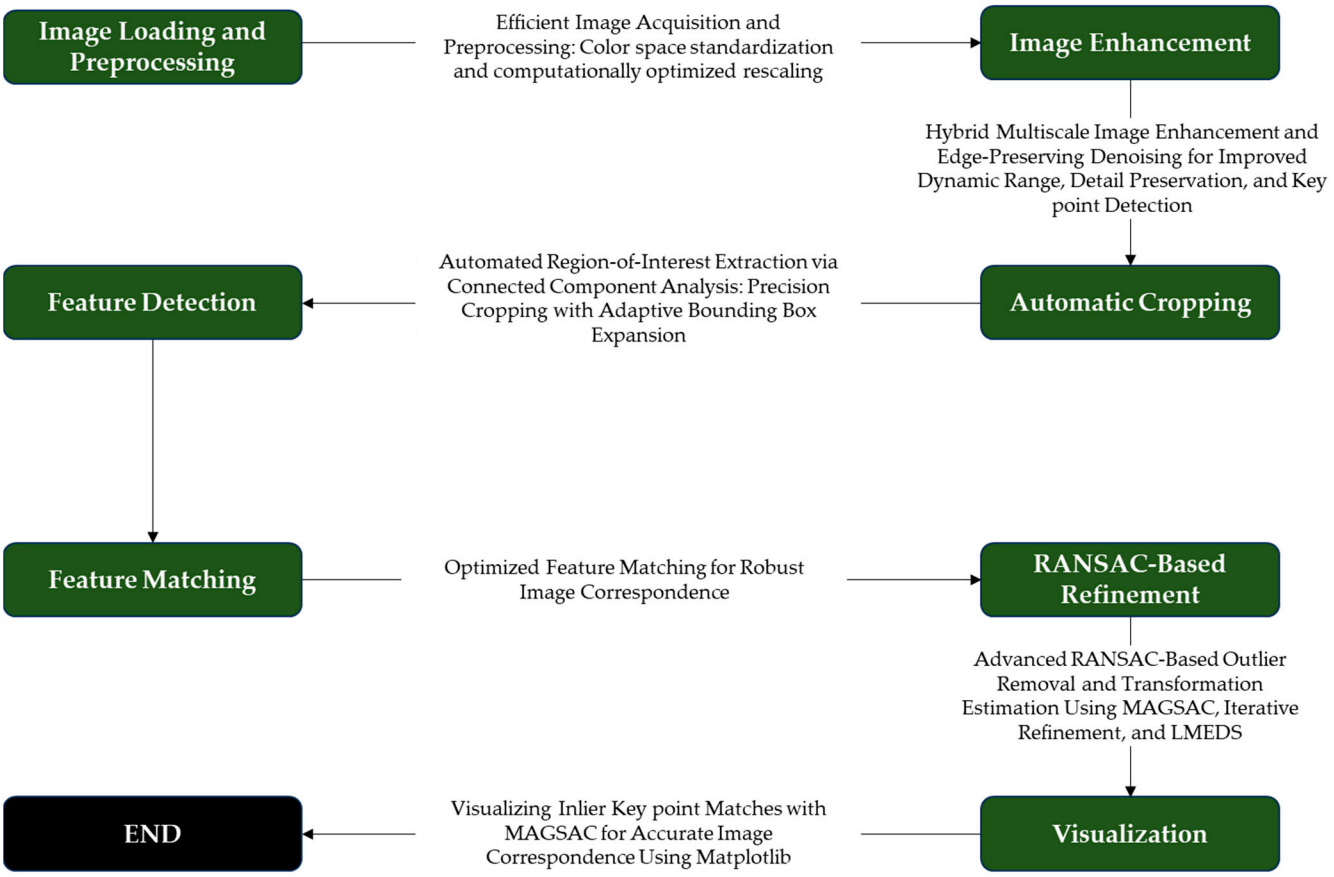


Figure 1. The block diagram of the proposed image processing pipeline.

Given an input image, I, with dimensions $m \times n \times 3$, the image is initially loaded and converted from BGR to RGB color space:

$$\boldsymbol{I_{RGB}} = cv2.cvtColor(I, cv2.Color_BGR2RGB) \tag{1}$$

The image is then resized by a scaling factor, s, adjusting its dimensions to optimize computational efficiency:

$$\boldsymbol{I_{resized}} = cv2.resize(\boldsymbol{I_{RGB}}, \ (sm, sn)) \tag{2}$$

3.3. Image Enhancement

At the image enhancement stage, multifaceted adaptive image enhancement is presented: integrating multiscale retinex, CLAHE, unsharp masking, wavelet denoising, bilateral filtering, and guided filtering for optimal detail and noise Reduction. At this stage, it aims to improve the quality of PTLI's image by enhancing details and reducing noise, facilitating better feature detection. Image enhancement is one of the important methods in this image processing, especially in PTLI images such as low lighting or complex backgrounds. The proposed image processing pipeline integrates several enhancement methods to maximize the visibility of key features. The first stage in this image enhancement is the integration of multiscale retinex (MSR) and contrast limited adaptive histogram equalization (CLAHE). MSR improves dynamic range and contrast by combining retinex operations on multiple scales, improving the visibility of details in light and dark regions. Meanwhile, CLAHE increases local contrast and makes details of different image regions more distinguishable. Unsharp masking is implemented to improve the edges by adding back a lower frequency of the original image and then averaging. The next step is the application of a sequence of filters, including a wavelet denoising filter, a bilateral filter, and

a guided filter. Wavelet denoising allows for the filtering out of noise so that small details and important information are not lost, while bilateral filtering smooths out the image while preserving edges. The final stage, with guided filtering, fine-tunes the refinement step and helps highlight the important features without producing any artifacts. The equation of the image enhancement process for multiscale retinex (MSR) for each pixel intensity $\boldsymbol{I_{resized}}\ (x, y)$ at position (x, y) is as follows:

$$\boldsymbol{R}(x, y) = \frac{1}{N} \sum_{i=1}^{n} (\log(\boldsymbol{I_{resized}}(x, y)) - \log(G_{\sigma i} * \boldsymbol{I_{resized}}(x, y))) \tag{3}$$

where $G_{\sigma i}$ is the Gaussian filter with scale σi, and n is the number of scales. The CLAHE operation is applied to the luminance channel $L(x, y)$ of the image in the LAB color space:

$$\boldsymbol{L_{\mathbf{CLAHE}}}(x, y) = \mathrm{CLAHE}(L(x, y)) \tag{4}$$

The sharpened image $\boldsymbol{I_{sharp}}$ is computed by:

$$\boldsymbol{I_{sharp}} = I_{CLAHE} + \lambda(I_{CLAHE} - I_{blurred}) \tag{5}$$

where $I_{blurred}$ is a Gaussian blurred version of I_{CLAHE}, and λ is a sharpening factor. Wavelet denoising is applied by decomposing the image into wavelet coefficients $W(I)$ and thresholding:

$$\boldsymbol{I_{denoised}} = W^{-1}\ (T(W(I))) \tag{6}$$

where T is a thresholding operator and W^{-1} is the inverse wavelet transform. The bilateral filter smooths the image while preserving edges:

$$\begin{aligned} \boldsymbol{I_{bilateral}}(x, y) = \tfrac{1}{W_p} \textstyle\sum_{(i,j)\in\boldsymbol{\Omega}} \boldsymbol{I_{denoised}}(i, j) \cdot exp\left(-\tfrac{(x-i)^2+(y-j)^2}{2\sigma_s^2} \right) \cdot \\ exp\left(-\tfrac{\left|\boldsymbol{I_{denoised}}(x,y)\boldsymbol{I_{denoised}}(x,j)^2\right|}{2\sigma_r^2} \right) \end{aligned} \tag{7}$$

where $\boldsymbol{\Omega}$ is the neighborhood of pixel (x, y), σ_s and σ_r are spatial and range parameters, and W_p is a normalization factor. Guided filtering further refines the image by:

$$\boldsymbol{I_{guided}} = GuidedFilter(\boldsymbol{I_{bilateral}}, \boldsymbol{I_{bilateral}}) \tag{8}$$

3.4. Automatic Cropping

Automatic cropping provides automatic methods for extraction of regions of interest (ROI) through connected components analysis with precision cropping with bounding boxes expanded adaptively. The goal of this stage is to eliminate areas of the image, which are not required to be further analyzed since this helps reduce the efficiency of the image analysis in this part. Thresholding is the first stage of automatic image cropping, which changes the image to a simpler format that highlights the ROI. Thus, the enhanced image stage is converted into grayscale for reduction of complexity as it eliminates the color channels and works only on the intensity values. The next step is binary and connected component analysis (CCA) where small blobs of pixels are detected and labeled based on their adjacency (i.e., connected region). Every connected area is considered an object. Following the execution of CCA, a process known as the bounding box stage is performed to identify the ROI's boundaries. Based on these calculations around this region, the most significant connected component, which is most probably the ROI, is chosen. Bounding refers to a rectangular frame that surrounds the entire component and maximizes the area of the image that sets the key regions of the image. The last stage of this stage is image cropping, where a number of regions within the image are cropped, with a view of eradicating unessential sections while retaining relevant information. The image is cropped based on the bounding box dimensions. This process eliminates backgrounds and focuses on the most important regions of the image. A small border is added to the bounding

box to ensure that no important details near the boundaries are lost during cropping. The equation for automatic cropping is as follows, where $\boldsymbol{T}(\boldsymbol{I})$ is the thresholded image:

$$\boldsymbol{T}(\boldsymbol{I}_{\boldsymbol{guided}}) = \begin{cases} 1 & if\ \boldsymbol{I}_{\boldsymbol{guided}}(x,y) > \boldsymbol{\tau} \\ 0 & otherwise \end{cases} \tag{9}$$

Connected component analysis identifies regions, and the bounding box $\boldsymbol{B}(x,y,w,h)$ is determined as follows:

$$\boldsymbol{B} = \text{BoundingBox}(\boldsymbol{T}(\boldsymbol{I}_{\boldsymbol{guided}})) \tag{10}$$

The image is cropped to this bounding box with a margin, δ, to retain key details:

$$\boldsymbol{I}_{\boldsymbol{cropped}} = \boldsymbol{I}_{\boldsymbol{guided}}(y-\delta : \text{y} + \text{h} + \delta, \text{x} - \delta : \text{x} + \text{w} + \delta) \tag{11}$$

3.5. Feature Detection

In this session, a hybrid feature extraction mechanism with the integration of ORB and SIFT was presented for enhanced scale-invariant, rotation-resilient key point detection and descriptor robustness. Feature detection is an important stage in the schematic flow proposed in this paper, as it involves identifying key points in the images that can be used to match two images. This image processing pipeline uses ORB (Oriented FAST and Rotated BRIEF) and SIFT (Scale-Invariant Feature Transform) algorithms for feature detection. ORB was chosen because of its efficient algorithm for detecting critical points and calculating binary descriptors, which can be optimized for real-time applications. This method is powerful for rotation and provides a fast binary descriptor. SIFT offers high accuracy in detecting and describing key points that are unchanged to scale, rotation, and partial lighting changes. The last stage is the merger of ORB and SIFT. This stage takes advantage of the speed of ORB and the robustness of SIFT, so it is expected to improve the detection toughness, increasing the possibility of accurate matching. Feature detection involves detecting key points $\{\boldsymbol{k}_i\}$ and their corresponding descriptors $\{\boldsymbol{d}_i\}$, key points $\{\boldsymbol{k}_{\boldsymbol{ORB}}\}$ and descriptors $\{\boldsymbol{d}_{\boldsymbol{ORB}}\}$ are computed using ORB:

$$\{\boldsymbol{k}_{\boldsymbol{ORB}},\ \boldsymbol{d}_{\boldsymbol{ORB}}\} = \text{ORB}(\boldsymbol{I}_{\boldsymbol{cropped}}) \tag{12}$$

Key points $\{\boldsymbol{k}_{\boldsymbol{SIFT}}\}$ and descriptors $\{\boldsymbol{d}_{\boldsymbol{SIFT}}\}$ are computed using SIFT:

$$\{\boldsymbol{k}_{\boldsymbol{SIFT}},\ \boldsymbol{d}_{\boldsymbol{SIFT}}\} = \text{ORB}(\boldsymbol{I}_{\boldsymbol{cropped}}) \tag{13}$$

The combined key points and descriptors are:

$$\{\boldsymbol{k}_{\boldsymbol{combined}}\} = \{\boldsymbol{k}_{\boldsymbol{ORB}}\} \cup \{\boldsymbol{k}_{\boldsymbol{SIFT}}\},\ \{\boldsymbol{d}_{\boldsymbol{combined}}\} = \{\boldsymbol{d}_{\boldsymbol{ORB}}\} \cup \{\boldsymbol{d}_{\boldsymbol{SIFT}}\} \tag{14}$$

3.6. Feature Matching

This feature matching session presents optimized key point correspondence through ORB and SIFT descriptor integration: dual-metric matching with Hamming distance, L2 Norm, and Lowe's Ratio test for enhanced accuracy. The feature-matching process applies to establishing a correspondence between the key points detected in two binocular images. The key point matching process used brute force matching. This technique compares the point descriptor from the first image with the point descriptor from the second image, and the best point match is identified based on the L2 norm distance. Lowe's ratio test is applicable to filter out inconsistent matches because it only considers the ratio of distance to the model and the next nearest model. The best point-matching parameters are those with point matches better than the second-best match by more than 0.75 times the distance value in the matching process. This method reduces the number of false point matches and increases the reliability of key point matching. The key point matchings are then ranked according to distance, where nearer distances represent closer feature point matching. This sorting process allows for prioritization of the most accurate key point matches before the

refinement stage. Feature matching is performed by finding correspondences between descriptors $\{\boldsymbol{d_{combined1}}\}$ from image $\boldsymbol{I_{cropped1}}$ and $\{\boldsymbol{d_{combined2}}\}$ from the image $\boldsymbol{I_{cropped2}}$; matches are found by minimizing the distance $\boldsymbol{d}$ between descriptors:

$$\boldsymbol{m_{i,j}} = \arg min_{i,j} \|\boldsymbol{d_{combined1}}(\boldsymbol{i}) - \boldsymbol{d_{combined2}}(\boldsymbol{j})\|_2 \tag{15}$$

Matches are filtered using Lowe's ratio test:

$$\text{Accept } \boldsymbol{m_{i,j}} \; if \; \frac{\|\boldsymbol{d_{combined1}}(\boldsymbol{i}) - \boldsymbol{d_{combined2}}(\boldsymbol{j})\|_2}{\|\boldsymbol{d_{combined1}}(\boldsymbol{i}) - \boldsymbol{d_{combined2}}(\boldsymbol{j'})\|_2} < \rho \tag{16}$$

where ρ is a predefined threshold, and $\boldsymbol{j'}$ is the second-closest match.

3.7. RANSAC-Based Outlier Removal

Random sample consensus (RANSAC)-based refinement presents an enhanced match refinement pipeline: m-estimator sample consensus (MAGSAC)-driven RANSAC optimization with iterative parameter tuning and LMEDS integration for superior outlier exclusion and transformation accuracy. To increase the accuracy of the key point matching, this image processing pipeline integrates a RANSAC-based refinement method. RANSAC is used to remove outliers from key point matching, where it randomly selects a subset of match points and estimates the model using only these points in each iteration. This image processing pipeline also involves key point matching using an algorithm known as MAGSAC, which is an enhancement of RANSAC. MAGSAC increases the precision of model estimation and accuracy of image alignment by eliminating outliers by dynamically estimating the threshold for inliers. At this point, it adjusts the RANSAC reprojection error threshold. RANSAC is run several times with different parameters, and the best match is selected to improve the durability of the matching process. In addition, the use of least median of squares (LMEDS) offers a good alternative for estimation especially when RANSAC is subjected to a certain noise or outlier. These refinement measures are critical to ensuring that the final set of key points matches is free of fake correspondence, leading to more accurate and reliable results at the next stage of analysis. Let $\boldsymbol{H}$ be the homography matrix that transforms points p_i from image $\boldsymbol{I_{cropped1}}$ to points $p_i{}'$ in image $\boldsymbol{I_{cropped2}}$. The MAGSAC approach minimizes the error between the transformed points while simultaneously estimating the optimal inlier threshold ϵ. The homography matrix $\boldsymbol{H}$ is determined by solving:

$$\boldsymbol{H} = \arg min_H \sum_{i=1}^{N} \rho(\|p_i' - Hp_i\|^2 \hat{\epsilon}) \tag{17}$$

where $\rho(\cdot, \hat{\epsilon})$ is the M-estimator cost function dependent on the dynamically estimated inlier threshold $\hat{\epsilon}$. MAGSAC modifies the RANSAC algorithm by estimating $\hat{\epsilon}$ during the model fitting, which ensures robustness against outliers.

3.8. Visualization

This session presents an improved correspondence visualization. In this stage, exclusive inlier key point mapping and Matplotlib representation are performed to ensure accurate match validation. Following the application of MAGSAC, the subsequent steps involve plotting the inlier's key points and showing the accurate key points in the scene. The Matplotlib is used to explain the key points matching where there is a representation of how the matching was conducted. This stage is crucial to ensure the accuracy of the match between the key points obtained and to get the relationship between the binocular images. The application of the color codes or connecting lines between the key point matching enhances the understandability of visualization in case the efficiency of key point

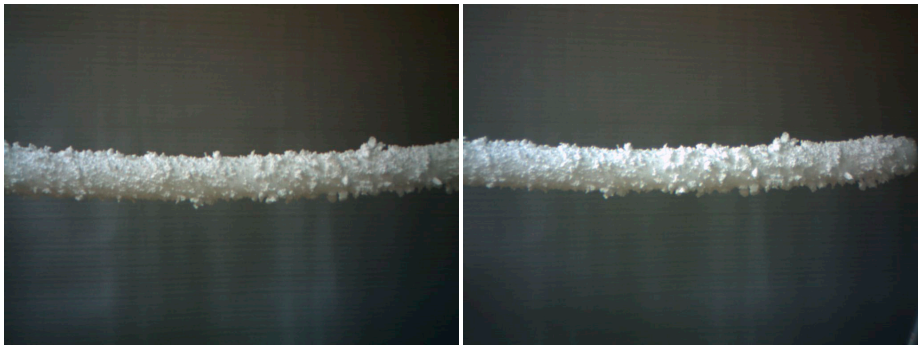
matching can be effectively assessed and explained. Finally, the inlier matches $\{\boldsymbol{m_{inliers}}\}$ are visualized by displaying the correspondences between images $\boldsymbol{I_{cropped1}}$ and $\boldsymbol{I_{cropped2}}$:

$$v = \boldsymbol{VisualizeInliers}\left(\boldsymbol{I_{cropped1}}, \boldsymbol{I_{cropped2}}, \{\boldsymbol{m_{inliers}}\}\right) \tag{18}$$

4. Experimental Setup

4.1. Dataset

The dataset used for this research was taken from our lab data, where the images consisted of a sequence of independently constructed scenes to simulate an ice-covered transmission line to facilitate the collection of PTLI imagery data. This research simulates the transmission line using long-cylinder pearl cotton (expandable polyethylene, EPE), EPE utilized in this study was sourced from Guangdong Chuanling New Material Technology Co., Ltd., located in Dongguan, China. Expanded polystyrene foam (EPS) is attached to the surface to simulate an ice load layer, EPS used in this study was sourced from Hebei Sashang Technology Co., Ltd., located in Shijiazhuang, China. The dataset in this research consists of 20 PTLI images taken randomly. PTLI images were collected using Daheng binocular cameras in a controlled indoor environment. The Daheng binocular cameras are manufactured by Daheng Imaging, based in Beijing, China. The image simulates a landscape covered in ice or a white sky. Figure 2 shows the PTLI image used for the experiment.



(**a**) (**b**)

Figure 2. PTLI image simulation (**a**) Left image; (**b**) Right image.

4.2. Evaluation Metrics

Evaluation metrics to assess the performance of image processing pipelines that focus on accuracy and practicality in PTLI imagery applications. The key point matching scheme proposed in this paper will be evaluated using a combination of quantitative, qualitative, and computational metrics, which are benchmarked against the traditional method. Key point matching accuracy is one of the critical metrics measured using the correct match ratio to the total number of key points detected. In addition, the accuracy of the 3D measurement of the ice thickness is evaluated by calculating the measurement error between the estimated 3D coordinates and the actual measurement. This evaluation is necessary in the case of ice thickness estimation, for which inaccuracies in measurements can result in deviations in the PTLI monitoring. Another criterion of the assessment of image processing pipelines is time complexity, which is applied to measure the time costs for detection, matching, and refinement of the key points necessary for the identification of relations to ensure that operations in these pipelines can be performed in real time. Finally, resistance to noise and varying lighting conditions were evaluated through comparative tests with traditional methods, determining how well the image processing pipeline in this study performed in a challenging environment. The traditional method will use the standard key point detection and matching techniques without the enhancements introduced in this paper.

4.2.1. Quantitative Metrics

Precision, recall, and F1 scores will be calculated to assess the accuracy and effectiveness of key point detection and key point matching in these evaluation metrics. These metrics can be computed using the matches and their validity as determined by the RANSAC refinement. Precision is employed to determine the ratio of the truth of all the matching key point coordinates detected to the total key point matches. This metric is to show how effective the correct match is from the wrong match compared to the baseline. Precision is the ratio of correctly matched key points (true positives) to the total number of points detected as a match (the sum of true positives and false positives). This metric provides insight into the accuracy of the proposed pipeline by measuring how many matching key points are correct.

$$\textbf{Precision} = \frac{\text{True positives(TP)}}{\text{True positives(TP)} + \text{False positives (FP)}} \tag{19}$$

- True Positives (TP): The count of correctly matched key points between images
- False positives (FP): The count of incorrect key point matches.

High precision means that most of the key points that are matched are correct, but it does not mean that all key points have been matched (ignoring missed matches).

Recall measures the proportion of true matches identified out of all possible true matches. A high recall means the method successfully captures most of the correct matches. It indicates how well the algorithm detects all the correct key points.

$$\textbf{Recall} = \frac{\text{True positives(TP)}}{\text{True positives(TP)} + \text{False negative (FP)}} \tag{20}$$

- False Negatives (FN): the count of key points that should have matched but were not detected (missed matches).

A high recall means that the algorithm finds most of the correct key points but may include some incorrect matches.

The F1 score is a measure derived from precision and recall that is the average of the two and that takes into consideration false positives and false negatives.

$$\textbf{F1 Score} = 2 \times \frac{\text{Precision} \times \text{Recall}}{\text{Precision} + \text{Recall}} \tag{21}$$

The F1 Score is a representative of the quality, where the maximum value is 1, while the minimum is 0, where 1 corresponds to the best result without error in both precision and recall.

4.2.2. Qualitative Evaluation

Quantitative analysis by visual assessment, which includes an analysis of the accuracy and efficiency of the detection and matching of the critical points on PTLI image. Key points are mapped onto the PTLI images to assess their accuracy, distribution, and relevance in terms of issues such as low light. Features points between the pairs of PTLI images are then compared to determine the accuracy of alignment, consistency, and reduction of false matches through line plots. This method helps determine the robustness of an image processing system compared to a baseline, especially in difficult environments and low light.

Key point detection on visualization is the result of the critical point detection that will be visualized on the image for a comprehensive examination. The objective is to evaluate the accuracy, distribution, and relevance of these key points matching between pairs of PTLI images. It is required to evaluate key factors such as:

- Density: How many critical points are detected throughout the image.
- Dispersion: The spread and coverage of points across different regions of the image.

- Effectiveness in challenging environments: Detection algorithm performance in low-light conditions.

These factors will be compared between the proposed image processing pipeline and the basic method for determining performance improvements, especially in detecting critical points in difficult lighting situations. Visualization on key point matching stage is the quality of the matching point between two pairs of PTLI images is visually assessed. Line plots are used to connect the corresponding key points in each PTLI image, allowing for visual comparison. Evaluation metrics include:

- Alignment Accuracy: The correlation between a given contribution of one image to the overall images and how well this related to the other in the other pairing relating to the image.
- False match reduction: the capability of the proposed pipeline to reduce the possibility of false match between the points.
- Consistency: The stability of feature matching of the key points in the images in different stages and scenes.

This comparison will be created with a baseline method, aiming to demonstrate improvements in alignment and match quality.

The qualitative evaluation will be conducted using images of the artificial PTLI under low-light conditions, emphasizing the robustness of the proposed pipeline in maintaining accurate key point detection and matching in such challenging environments.

4.2.3. Computational Efficiency

Based on time, computational efficiency estimates how a pipeline of image processing for detecting and matching crucial points takes. This evaluation will be documented and then compared with the conventional methods that have been used. The part and parcel of this process is key point detection and matching. The time needed for the identification of the critical points through ORB or SIFT, then checking for the correspondence through the Lowe's ratio test and then applying the RANSAC to refine the result. An evaluation will be made to analyze the trade-off between achieving higher accuracy and overall computation time concerning PTLI's image dataset.

4.2.4. Application to Ice Thickness Measurement

The pipeline application proposed in this paper is for ice thickness measurement on PTLI, which will be evaluated through several main metrics. The accuracy of the pipeline in 3-D measurements and ice thickness measurements compared to traditional methods. The results will be validated against ice thickness measurements using manual measurements of micrometers (ground truth) to assess the improvement in precision and accuracy. This comprehensive evaluation aims to explain the advantages of this pipeline in terms of precision, recall, and computational efficiency, especially in PTLI images where accurate ice thickness measurement is necessary for monitoring on PTLI.

4.3. Experimental Procedure

The experimental procedure involves a detailed description of the settings, software environment, and hardware specifications used during the evaluation.

- Setup The experimental setup includes a controlled environment for processing PTLI images. The PTLI image dataset includes images taken under various lighting conditions and ice accumulation scenarios on power transmission lines. The images will be pre-processed and further improved through the application of the proposed pipeline for key point detection and 3D reconstruction.
- Software environment: The experiment software includes OpenCV 4.0 image processing libraries, and it uses the Python 3.11 platform to develop key point detection and matching algorithms including ORB, SIFT, and Lowe's ratio test. Metrics for evalua-

tion and analysis will be based on Python, which includes tools for visual inspection, 3D reconstruction, and computation performance measurement.

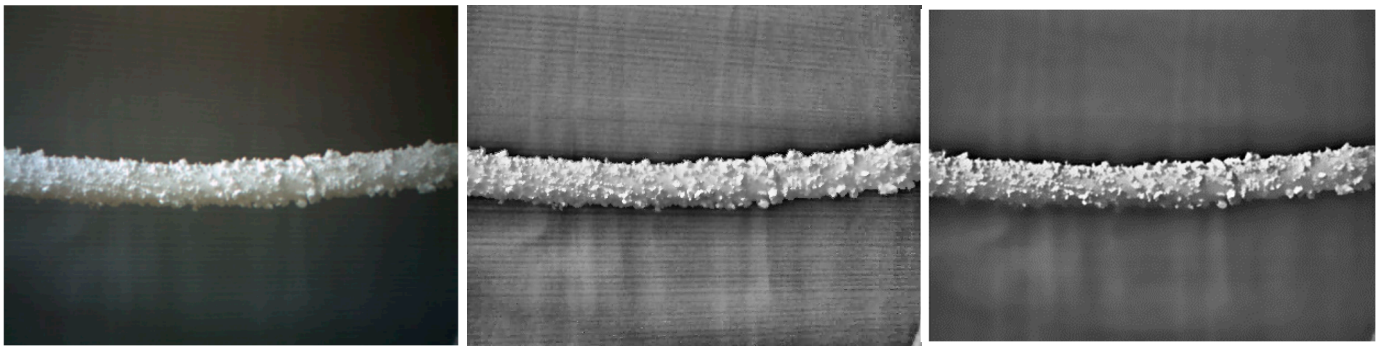
- Hardware specs: The experiment will be performed on a high-performance workstation with a multi-core processor (Intel i9) having at least 32 GB of RAM to deal with PTLI image dataset. The multi-core processor used in this study is the Intel i9, manufactured by Intel Corporation, located in Santa Clara, California, USA for key point detection, matching and 3D reconstruction. NVIDIA Corporation, located in Santa Clara, California, USA are employed to accelerate the process. As for storage, SSDs are used in order to have fast and efficient data storage and retrieval.

This experimental procedure ensures that the experiment is conducted in an optimal environment to accurately measure performance, computing efficiency, and accuracy.

5. Results and Discussion

5.1. Performance of the Image Enhancement Techniques and Automatic Cropping

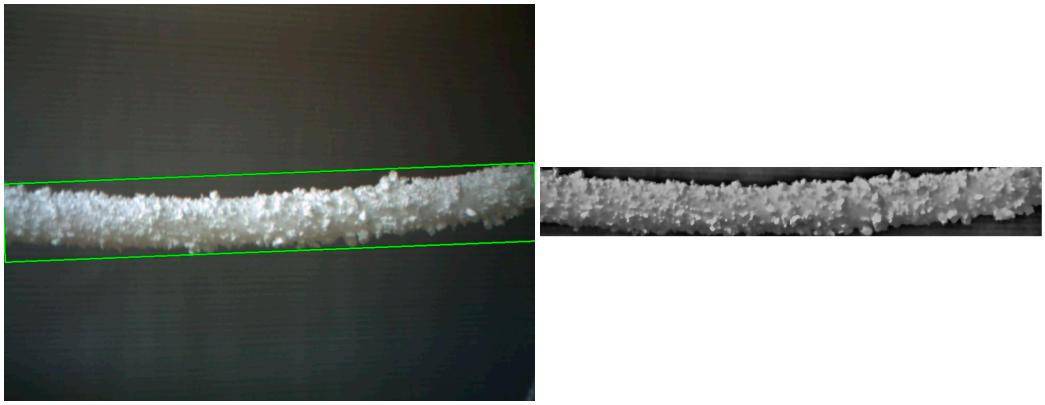
This session aims to demonstrate the success of improving the quality of PTLI images to improve the visibility of the ice load and facilitate 3D reconstruction. In addition, the result of automatic cropping was also shown in this session. Automatic cropping searches for regions of interest and removes unnecessary areas. Figure 3 shows the results of image enhancement.



(**a**) (**b**) (**c**)

Figure 3. Performance of image enhancement techniques and automatic cropping. (**a**) Original image; (**b**) Image enhancement; (**c**) Image denoising.

Figure 3 demonstrates the performance of the image enhancement techniques and the automatic cropping process. In Figure 3a, the original PTLI image is shown as a baseline. Figure 3b displays the enhanced image, where visibility and contrast are improved through the applied image enhancement techniques. Finally, Figure 3c illustrates the results after image denoising on the PTLI image, where noise has been reduced while preserving important details for further analysis. Figure 4 illustrates the automatic cropping process applied to a PTLI image. In Figure 4a, the framing of the region of interest (ROI) shows how the relevant portion of the image is identified before automatic cropping is performed. Figure 4b presents the results after the automatic cropping has been completed to the PTLI image, where unnecessary background elements have been removed, focusing on the key area for further image analysis.



(**a**) (**b**)

Figure 4. Automatic cropping process on PTLI image. (**a**) The process of framing the region of interest before automatic cropping is conducted. (**b**) The results of automatic cropping.

5.2. Key Point Detection and Matching Accuracy

The accuracy of key point detection and matching is analyzed by comparing the ORB, SIFT, ORB2, and the proposed methods in this paper. The accuracy is calculated using precision, recall, and F1 score in Equations (19)–(21). In this experiment, 20 PTLI images were taken at random. Figure 5 shows the precision comparison graph of several methods.

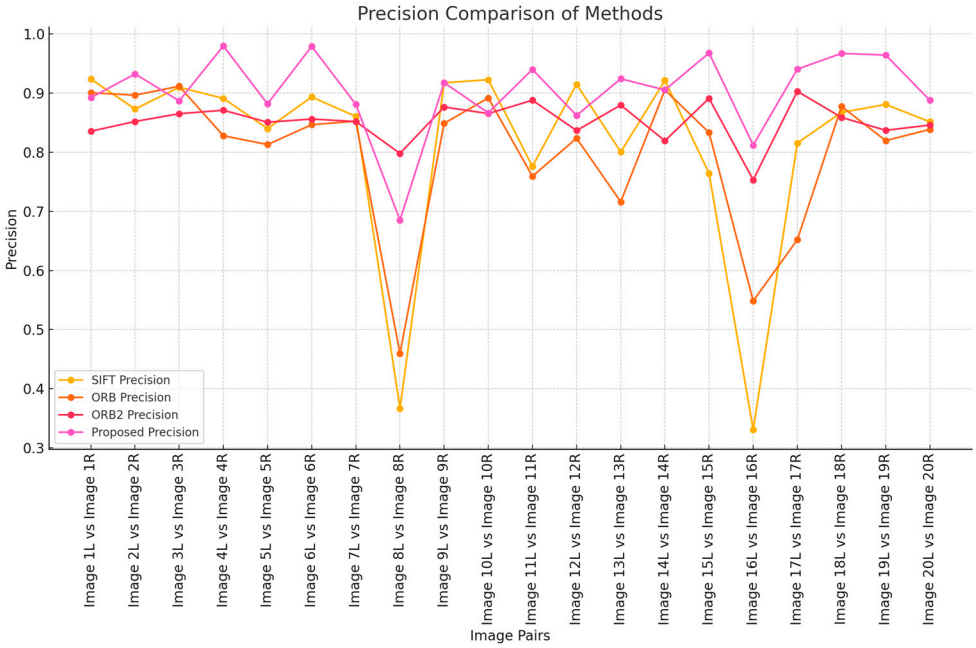


Figure 5. The precision comparison graph of several methods.

The performance results of each method of accuracy calculation using precision in Equation (12) have been shown in Figure 5. Based on Figure 5, the proposed method consistently demonstrates superior precision in most image pairs. The average precision of the proposed method is 90%, the highest average precision among other methods. SIFT and ORB2 have an average precision value of around 82% and 85%, respectively. The precision values of the two methods are still below the proposed method. The lowest precision value is the ORB method, which only has an average precision of 80%. Figure 6 shows the recall comparison graph of several methods.

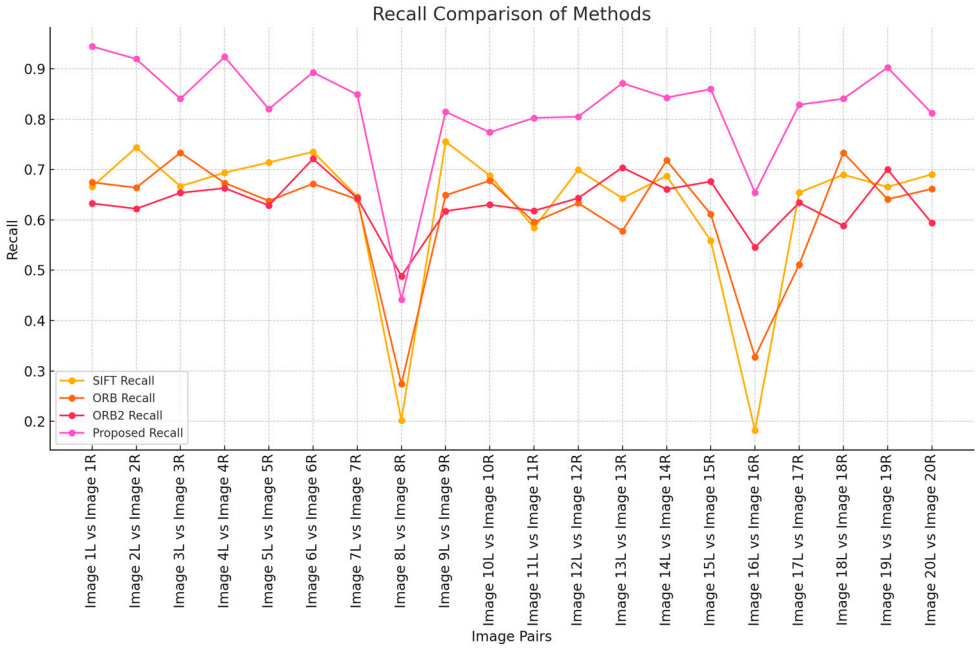


Figure 6. The recall comparison graph of several methods.

The recall values of all methods are presented in Figure 6 above. As can be seen in Figure 6, the proposed method gives the highest average recall value, which is 82 percent. This average recall shows that it has been more successful in detecting and matching relevant key points than other methods. The average recall values for SIFT, ORB, and ORB2 only ranged from 62–63%, indicating that several key points were not successfully detected or matched on several pairs of PTLI images. Figure 7 shows the F1 score graph of several methods.

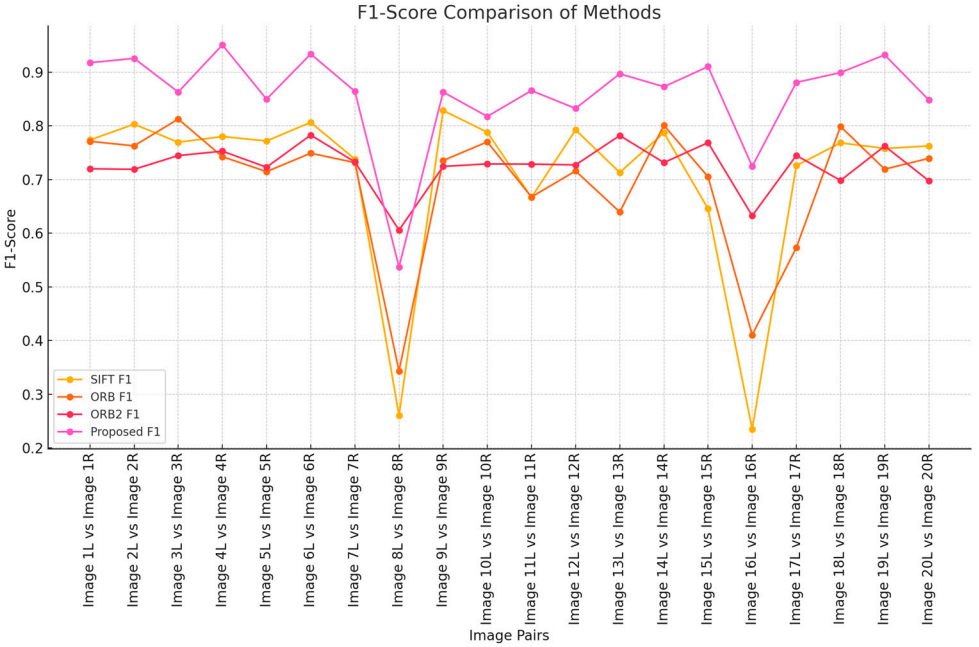


Figure 7. The F1 score graph of several methods.

A comparison of the F1 scores from several methods for the detection of key points and pairs has been shown in Figure 7. The F1 score is a precision and recall balancer, based on Figure 7, which is shown to be the highest achieved by the proposed method, with an

average F1 score of 86%. ORB2 ranks second with an average F1 score of 73%. SIFT and ORB have the lowest F1 score of the proposed method and ORB at only around 71–70%.

Based on Figure 5, particularly in image pair number 8 (Image 8L and Image 8R) and number 16 (Image 16L and Image 16R), as well as in Figures 6 and 7, a striking difference in results among the other image pairs can be observed. The causes of degradation in these PTLI images are mainly related to environmental factors that affect key point detection and matching accuracy. In particular, image pairs numbers 8 and 16 show problems with low contrast due to low illumination conditions, resulting in fewer key points being detected, which interferes with accurate key point matching and reduces overall matching performance. For image pair number 8 and 16 of PTLI images, the lowest precision and recall values are held by the SIFT method, with a precision value of 36% and recall with a value of 20%. The best performance is shown by the ORB2 method with a precision value of 79%, but it is still categorized as medium precision. The proposed method also experienced difficulties in identifying the key points in the number 8 image pair, where the precision value was only 40%, even though the average precision was 90%. The image pair that shows the best performance on all key point detection and matching methods is number 6 (Image 6L vs. Image 6R). The proposed method has a precision of 90%, which leads to an F1 score of 93.4% in image pair number 6. The best performance on the proposed method was also shown in the number pairs of number 17 and 19, in which the number pairs reached 90% on all metrics.

Based on Figures 5–7, a conclusion can be drawn from comparing all methods for key point detection and matching. The advantage of the proposed method is that it is more consistent in almost all PTLI image pairs. The advantages of this method are shown in all metric values, namely precision, recall, and F1 scores, for all methods. The proposed method has a better balance between precision and recall among all other methods, which indicates that this method has the highest F1 score. Meanwhile, ORB2 is generally better than ORB in some pairs of PTLI images, especially in the average precision value. The average recall value almost shows comparable values between the two, but ORB2 is better overall, especially in the analysis using F1. SIFT is a traditional method for detecting and matching key points, so based on the analysis using metrics in Equations (19)–(21), the value is the lowest among the ORB2 method and the proposed method in most cases in PTLI image pairs. Therefore, SIFT has made many mistakes in the key point matching process. Summary statistics for the methods table are shown in Table 1.

Table 1. Summary statistics for methods.

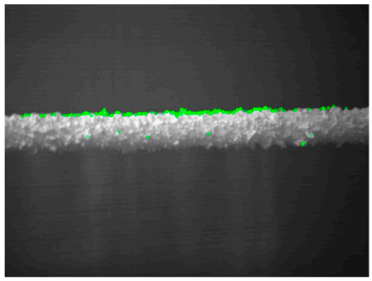
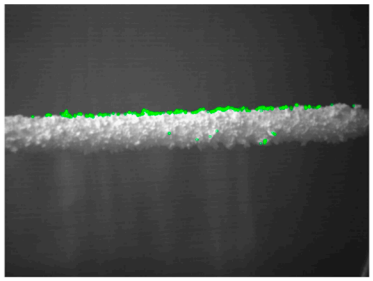
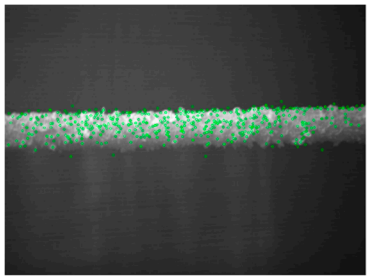
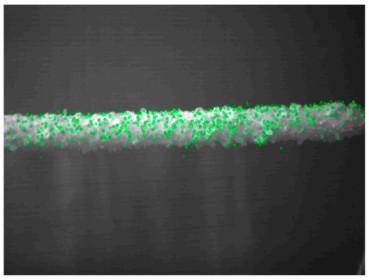
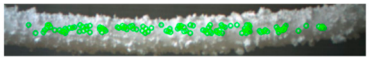
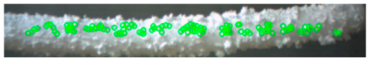
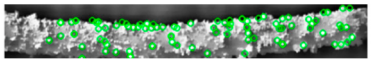
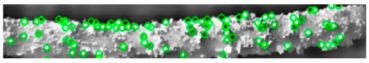
Metric	SIFT Mean	SIFT StdDev	ORB Mean	ORB StdDev	ORB2 Mean	ORB2 StdDev	Proposed Mean	Proposed StdDev
Precision	0.816116	0.16706	0.80121	0.121075	0.851805	0.034071	0.903738	0.068145
Recall	0.628211	0.156541	0.615325	0.119644	0.633162	0.053434	0.821928	0.109546
F1 Score	0.708776	0.163991	0.695254	0.122904	0.725497	0.043461	0.859413	0.091229

Based on Table 1, the highest average values across all metrics (precision, recall, and F1 score) were achieved by the proposed method. This proposed method has a relatively low variability (standard deviation), so it shows reliable and consistent performance. ORB2 occupies the precision value and F1 score number two of all methods. Then, lower average performance and higher variability, especially in recall, are shown by the SIFT and ORB methods.

Performance of the Key Point Detection and Key Point Matching

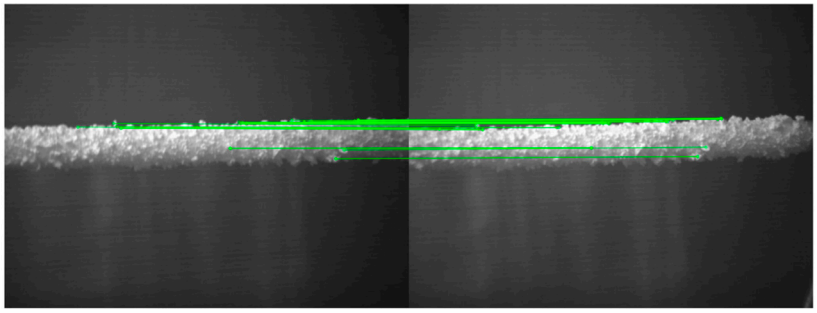
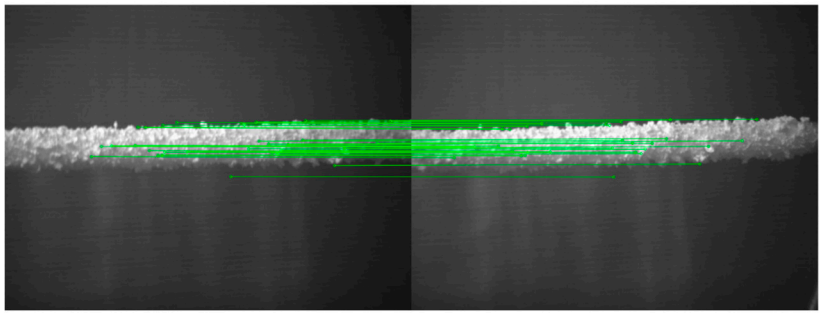
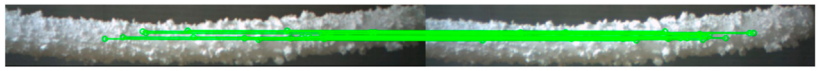
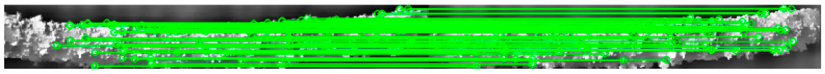
In this subsection, key point detection and matching results from all methods are visualized. This visualization provides a thorough assessment of the feature extraction technique's effectiveness and accuracy. Table 2 shows the results of key point detection from all methods.

Table 2. The results of key point detection from all methods.

Method	Result	
ORB		
SIFT		
ORB2		
Proposed Method		

Based on Table 2, key points are successfully detected on the structured surfaces indicated by the ORB method. In the image pair, the key points (visualized with green dots) are distributed in the structured area of the pattern and focus only on the higher contrast areas. In contrast, the low-contrast areas cannot be detected by this method. It can be concluded that the ORB method can detect key points in the structured region, but this method has difficulty with changes in illumination. In Table 2, it can be seen that the ORB only captures the key point on the top edge. ORB2 shows a wider area of detected key points. The increased detection of key points (visualized using green dots) in the area that has been successfully cut shows that this method is better than ORB. In this method, the cropped parts show that it is also successful in detecting key points in smooth structures or higher contrast differences more clearly, but grouping in certain areas can indicate limitations in detecting features with the same distance in this method. The original image that has been enhanced and cropped to speed up image processing in the proposed method affects improvements of the key point detection results. Based on Table 2, the pair of images using the proposed method produces more accurate key points. The images in the table show that the location of the key point detection in the right and left images is almost the same as in the PTLI area. Compared to other methods, this proposed method has a higher fit between the right and left images. The density of key points in the PTLI area is more even; the low contrast area can also be detected so that the proposed method shows better performance for PTLI images that require feature correspondence. Based on Table 2, the SIFT method detects more key points, but its accuracy is lower. There is a point mismatch in the right and left image pairs: a key point is detected in the right image but not in the left image, and so on. Table 3 shows the results of key point matching from all methods.

Table 3. The results of key point matching from all methods.

Method	Result
ORB	
SIFT	
ORB2	
Proposed Method	

Based on Table 3, the key point matching between PTLI image pairs is shown with a green line. In the ORB method, the key point matching is located in the central texture, which shows that the ORB method can only detect and match high-contrast features. The number of key point matches in this method is less than in other methods, which means that ORB has limitations when dealing with low-texture regions. SIFT can generally detect and match more key points than ORBs. However, SIFT also detects areas that are not needed. When compared to ORB, SIFT is stable. ORB2 is an improvement from the ORB method. For this method improvement, the areas that are needed are highlighted and those that are not needed are cropped. In this method, the number of key point matching is more than that of traditional ORB; the improvement focuses on a smaller area and image enhancement. This method is successfully applied to imagery with strong gradients but may fail to capture complex or more subtle features. The proposed method significantly increases the number of key point matches compared to other methods. Key point matching in the proposed method is more even and consistent. Table 3 shows many key points that are accurately matched across the entire surface of the object. In addition, this method is reliable in handling smooth texture images and also low contrast or changes in illumination.

5.3. Analysis of Computational Efficiency for Key Point Detection and Matching

The overall efficiency of the method for key point detection and key point matching is evaluated by measuring the processing time for key point detection and key point matching. Figure 8 shows the processing times for key point detection and key point matching of all methods.

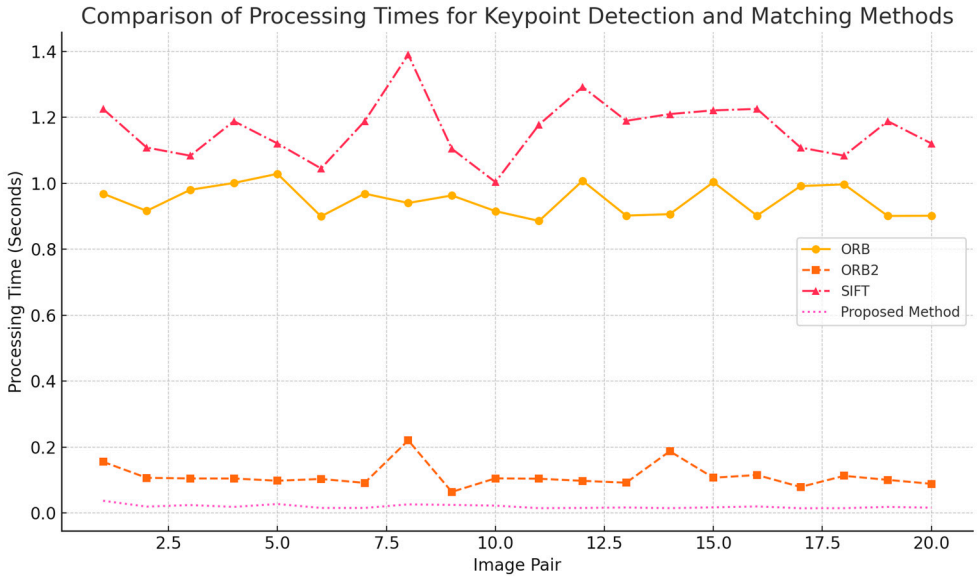


Figure 8. The processing times for key point detection and key point matching of all methods.

The processing time of four methods (ORB, ORB2, SIFT, and proposed method) for key point detection and matching in 20 pairs of images are visually compared in Figure 8. Based on Figure 8, the longest processing time shown is by the SIFT method, and the average processing time is 1 s more on most PTLI image pairs. The SIFT line graph shows the longest processing time of about 1.4 s in several pairs of PTLI images. The ORB method shows the second-longest processing time after SIFT. Some image pairs reach 1 s, with small fluctuations across image pairs, so, ORB is more efficient than the SIFT method. Based on the analysis of Figure 8, it is shown that ORB2 is better than SIFT and ORB, with an average processing time of 0.1 s. The fastest processing time, among other methods, is the proposed method. It consistently takes an average of 0.01 s, making it the most efficient method with a significant margin among other methods. In addition, this method is ideal if applied in real time.

5.4. Application to 3D Measurement and Ice Thickness Estimation

The proposed key point detection and matching methods are tested for their performance in applying 3D measurements for ice thickness for PTLI imagery. Table 4 shows the results of applying the proposed method to 3D measurements for ice thickness on PTLI. This paper focuses only on the application of key point matching in 3D measurement. The 3D measurement is used here only to verify the performance of key point matching for ice thickness measurements in transmission lines. A micrometer is used for manual measurements that will be used for ground truth. In this measurement, SIFT [31] and ORB2 [2] are used for comparison. Finally, the proposed method is compared with other methods for applying 3D measurements for ice thickness for PTLI images.

Table 4. The results of applying the proposed method to 3D measurements for ice thickness on PTLI.

Measurement Location	**1**	**2**	**3**	**4**	**5**	**6**	**7**	**8**	**9**	**10**	**11**	**12**	**13**	**14**	**15**
Manual (mm)	88.5	90.4	88.7	77.4	81.8	81.4	79.6	82.8	80.6	80.7	86.8	72.7	80.2	79.5	79.8
SIFT [31] (mm)	100.2	100.8	98.4	88.3	93.7	95.1	86.8	95.2	83.1	98.2	90.6	87.3	91.1	88.7	90.3
ORB2 [2] (mm)	89.8	92.7	86.8	80.7	83.1	83.7	78.9	85.1	77.3	83	89.1	75.3	83.5	81.8	78.2
Proposed method (mm)	87	92.2	89.3	76	81.2	82	80.1	83.5	79.3	79.1	88.6	71.9	81.9	78.7	80.6
Absolute error	1.5	1.8	0.6	1.4	0.6	0.6	0.5	0.7	1.3	1.6	1.8	0.8	1.7	0.8	0.8

Table 4 shows the results of manual measurements used for ground truth on the thickness of the ice on the power transmission line. Measurement results using the SIFT method result in higher measurements than manual measurements; in some cases, the PTLI image has a large deviation (e.g., 100.2 mm vs. 88.5 mm for Location 1). The measurements using the ORB2 method present results closer to manual measurements when compared to the SIFT method, but some cases still show significant differences. The proposed method successfully provides more accurate measurements, which are very close to the results of manual measurements at most PTLI locations. As in the absolute error column, where the error ranges from 0.55–1.8 mm. Based on Table 4 regarding the absolute error between the proposed method and the manual measurement, it is mostly low. This method indicates that the proposed method has a good performance in the ice thickness measurement on the PTLI. The most significant error was at location 11, which was 1.8 mm. However, the overall average error is below 2 mm, which indicates that the proposed method is more reliable and accurate than other methods.

The findings of this study have significant implications for PTLI. The capabilities of the proposed method are to improve image quality and the accuracy of direct key point detection on better monitoring of power lines, especially in challenging environments with dim or complex light backgrounds. The efficiency of this method in terms of processing time is excellent for real-time monitoring and maintenance, which can potentially improve the reliability and safety of the power transmission system. In addition, precise 3D measurement capabilities can be instrumental in measuring ice loads on transmission lines, which is crucial for preventing line damage or service interruptions.

Despite the success of the proposed method, some limitations must be acknowledged. First, the PTLI image resolution may limit the accuracy of key point detection in some cases, especially in areas with low contrast. Additionally, while processing time is significantly reduced, further improvements are required to ensure scalability across large datasets or higher-resolution imagery without sacrificing accuracy. The method's performance can also be affected by drastic changes in lighting or texture, where further adjustments may be required. The accuracy also needs to be improved.

Future research may focus on several avenues to improve the proposed image processing methods. One promising area is optimizing methods for faster processing times, ensuring scalability for large-scale industrial applications. Another direction could involve exploring these methods outside of power transmission lines, such as aerial inspections of other critical infrastructure, such as bridges or pipelines. In addition, integrating real-time monitoring capabilities, potentially through drones or automated systems, can significantly improve the application of pipelines in real-world scenarios.

6. Conclusions

The proposed method significantly improves the image enhancement key point detection and matching processes, especially for PTLI images. Image enhancement techniques result in better visibility in low-light conditions and successful noise reduction while retaining important details. In addition, the automatic cropping method effectively isolates the region of interest, removing unnecessary areas and speeding up the overall image processing. Key point detection and matching are also enhanced with the proposed method, which consistently outperforms traditional methods such as SIFT and ORB regarding precision, recall, and F1 score, with an average precision of 90% and an F1 score of 86%. Pipe computing efficiency reduces processing time to as low as 0.01 s, making it feasible for real-time applications. Finally, the proposed method can provide accurate 3D measurements of the thickness of the ice on the power transmission line, with an absolute error of less than 2 mm compared to manual measurements.

Author Contributions: The ideas and concepts were carried out in collaboration with all authors. N.R.N. and J.X. conceived and designed the experiments; N.R.N. and X.H. performed the experiments; N.R.N. and J.X. analyzed the data; N.R.N. and J.X. wrote the paper. All authors have read and agreed to the published version of the manuscript.

Funding: This research received no external funding.

Data Availability Statement: The original contributions presented in the study are included in the article, further inquiries can be directed to the corresponding author.

Conflicts of Interest: The authors declare no conflicts of interest.

References

1. Han, S.; Li, D.; Li, K.; Wu, H.; Gao, Y.; Zhang, Y.; Yuan, R. Analysis and Study of Transmission Line Icing Based on Grey Correlation Pearson Combinatorial Optimization Support Vector Machine. *Measurement* **2024**, *236*, 115086. [CrossRef]
2. Nusantika, N.R.; Hu, X.; Xiao, J. Newly Designed Identification Scheme for Monitoring Ice Thickness on Power Transmission Lines. *Appl. Sci.* **2023**, *13*, 9862. [CrossRef]
3. Wen, Y.; Wu, J.; Gao, Z.; He, J.; Li, H.; Gong, B. Transmission Line Icing Forecasting Based on Characteristic Graph Structure. In Proceedings of the Second International Conference on Digital Society and Intelligent Systems (DSInS 2022), Chendgu, China, 2–4 December 2022; pp. 236–244, ISBN 9781510663244.
4. Pan, H.; Zhou, F.; Ma, Y.; Ma, Y.; Qiu, P.; Guo, J. Multiple Factors Coupling Probability Calculation Model of Transmission Line Ice-Shedding. *Energies* **2024**, *17*, 1208. [CrossRef]
5. Wang, G.; Shen, J.; Jin, M.; Huang, S.; Li, Z.; Guo, X. Prediction model for transmission line icing based on data assimilation and model integration. *Front. Environ. Sci.* **2024**, *12*, 1403426. [CrossRef]
6. Shen, H.; Wan, B.; Zhou, S.; Kang, J.; Chen, H.; Gao, Z. The Synoptic Characteristics of Icing Events on Transmission Lines in Southern China. *Atmosphere* **2023**, *14*, 1789. [CrossRef]
7. Chen, Q.; Liu, T.; Wang, Z.; Miao, R. Research on monitoring method for ice-covered state of transmission lines based on conductor end displacement. *Electr. Power Syst. Res.* **2024**, *236*, 110918. [CrossRef]
8. Liu, Z.; Song, B.; Guo, Y.; Xu, H. Improved Template Matching Based Stereo Vision Sparse 3D Reconstruction Algorithm. In Proceedings of the 32nd Chinese Control and Decision Conference (CCDC), Hefei, China, 22–24 August 2020.
9. Zhang, L.; Cai, F.; Wang, J.; Lv, C.; Liu, W.; Guo, G.; Liu, H.; Xing, Y. Image Matching Algorithm Based on ORB and K-Means Clustering. In Proceedings of the 2020 5th International Conference on Information Science, Computer Technology and Transportation (ISCTT), Shenyang, China, 13–15 November 2020; pp. 460–464.
10. Cong, L.; Huang, C.; Sui, J.; Dou, Z.; Li, J.; Li, Y.; Han, Z. Cable Fault Detection And Extraction Based on UAV Collected Images. In Proceedings of the 2022 International Conference on Computing, Communication, Perception and Quantum Technology (CCPQT), Xiamen, China, 5–7 August 2022; pp. 383–389.
11. Weng, B.; Gao, W.; Zheng, W.; Yang, G. Newly Designed Identifying Method for Ice Thickness on High-Voltage Transmission Lines via Machine Vision. *High Volt.* **2021**, *6*, 904–922. [CrossRef]
12. Nusantika, N.R.; Xiao, J.; Hu, X. New Scheme of Image Matching for The Power Transmission Line Icing. In Proceedings of the ICIEA 2022 17th IEEE Conference on Industrial Electronics and Applications, Chengdu, China, 16–19 December 2022; pp. 1–7.
13. Yang, Z.; Yang, L.; Chen, G.; Yap, P.-T. Improved polar complex exponential transform for robust local image description. *Pattern Recognit.* **2023**, *143*, 109786. [CrossRef]
14. Ramadan, M.; El Tokhey, M.; Ragab, A.; Fath-Allah, T.; Ragheb, A. Adopted Image Matching Techniques for Aiding Indoor Navigation. *Ain Shams Eng. J.* **2021**, *12*, 3649–3658. [CrossRef]
15. Lozano-Vázquez, L.V.; Miura, J.; Rosales-Silva, A.J.; Luviano-Juárez, A.; Mújica-Vargas, D. Analysis of Different Image Enhancement and Feature Extraction Methods. *Mathematics* **2022**, *10*, 2407. [CrossRef]
16. Bao, J.; Yuan, X.; Huang, G.; Lam, C.T. Point Cloud Plane Segmentation-Based Robust Image Matching for Camera Pose Estimation. *Remote Sens.* **2023**, *15*, 497. [CrossRef]
17. Bay, H.; Ess, A.; Tuytelaars, T.; Van Gool, L. Speeded-Up Robust Features (SURF). *Comput. Vis. Image Underst.* **2008**, *110*, 346–359. [CrossRef]
18. Lowe, D.G. Distinctive Image Features from Scale-Invariant Keypoints. *Int. J. Comput. Vis.* **2004**, *60*, 91–110. [CrossRef]
19. Yan, Z.; Wang, H.; Ning, Q.; Lu, Y. Robust Image Matching Based on Image Feature and Depth Information Fusion. *Machines* **2022**, *10*, 456. [CrossRef]
20. Leutenegger, S.; Chli, M.; Siegwart, R.Y. BRISK: Binary Robust Invariant Scalable Keypoints. In Proceedings of the IEEE International Conference on Computer Vision, Barcelona, Spain, 6–13 November 2011; pp. 2548–2555, ISBN 9781457711015.
21. Kim, Y.-J.; Son, D.-M.; Lee, S.-H. Retinex Jointed Multiscale CLAHE Model for HDR Image Tone Compression. *Mathematics* **2024**, *12*, 1541. [CrossRef]
22. Li, D.; Zhou, J.; Wang, S.; Zhang, D.; Zhang, W.; Alwadai, R.; Alenezi, F.; Tiwari, P.; Shi, T. Adaptive Weighted Multiscale Retinex for Underwater Image Enhancement. *Eng. Appl. Artif. Intell.* **2023**, *123*, 106457. [CrossRef]
23. Szabó, K.; Erdei, L.; Bolla, B.S.; Tax, G.; Bíró, T.; Kemény, L. Factors Shaping the Composition of the Cutaneous Microbiota. *Br. J. Dermatol.* **2017**, *176*, 344–351. [CrossRef]
24. Matin, F.; Jeong, Y.; Park, H. Retinex-Based Image Enhancement with Particle Swarm Optimization and Multi-Objective Function. *IEICE Trans. Inf. Syst.* **2020**, *103*, 2721–2724. [CrossRef]

25. Pizer, S.M.; Austin, J.D.; Perry, J.R.; Safrit, H.D.; Zimmerman, J.B. Adaptive Histogram Equalization for Automatic Contrast Enhancement of Medical Images. In *Application of Optical Instrumentation in Medicine XIV and Picture Archiving and Communication Systems*; Spie: Bellingham, WA, USA, 1986; pp. 242–250. Available online: https://www.spiedigitallibrary.org/conference-proceedings-of-spie/0626/0000/Adaptive-Histogram-Equalization-For-Automatic-Contrast-Enhancement-Of-Medical-Images/10.1117/12.975399.short (accessed on 27 October 2024).
26. Pisano, E.D.; Zong, S.; Hemminger, B.M.; DeLuca, M.; Johnston, R.E.; Muller, K.; Braeuning, M.P.; Pizer, S.M. Contrast Limited Adaptive Histogram Equalization Image Processing to Improve the Detection of Simulated Spiculations in Dense Mammograms. *J. Digit. Imaging* **1998**, *11*, 193–200. [CrossRef]
27. Li, H.; Wang, S.; Li, S.; Wang, H.; Wen, S.; Li, F. Thermal Infrared-Image-Enhancement Algorithm Based on Multi-Scale Guided Filtering. *Fire* **2024**, *7*, 192. [CrossRef]
28. Nusantika, N.R.; Hu, X.; Xiao, J. Improvement Canny Edge Detection for the UAV Icing Monitoring of Transmission Line Icing. In Proceedings of the 16th IEEE Conference on Industrial Electronics and Applications (ICIEA), Chengdu, China, 1–4 August 2021; pp. 1838–1843.
29. Wang, J.; Wang, J.; Shao, J.; Li, J. Image Recognition of Icing Thickness on Power Transmission Lines Based on a Least Squares Hough Transform. *Energies* **2017**, *10*, 415. [CrossRef]
30. Li, H.; Chen, Y.; Zhang, G.; Li, J.; Zhang, N.; Du, B.; Liu, H.; Xiong, N. Transmission Line Ice Coating Prediction Model Based on EEMD Feature Extraction. *IEEE Access* **2019**, *7*, 40695–40706. [CrossRef]
31. Guo, Q.; Hu, X. Power Line Icing Monitoring Method Using Binocular Stereo Vision. In Proceedings of the 2017 12th IEEE Conference on Industrial Electronics and Applications (ICIEA), Siem Reap, Cambodia, 18–20 June 2018; pp. 1905–1908.

Disclaimer/Publisher's Note: The statements, opinions and data contained in all publications are solely those of the individual author(s) and contributor(s) and not of MDPI and/or the editor(s). MDPI and/or the editor(s) disclaim responsibility for any injury to people or property resulting from any ideas, methods, instructions or products referred to in the content.